

Computation of the Thermodynamics, Structural and Transport Properties of Liquid Methane by Isothermal-Isobaric Molecular Dynamics

N. Tchouar^{1*}, F Ould-Kaddour² and M. Benyettou¹

¹Laboratory of Modelisation of Industrial Systems, Faculty of Science, U.S.T.O, P.O.Box BP 1505 El Menaour, Oran-Algeria. Fax : 21341420680. e-mail: lamosi2002@yahoo.fr

²Dept. of Physics, Faculty of Science, Univerity Abou-Bekr Belkaid of Tlemcen, Tlemcen-Algeria.

Abstract: The Properties of liquid methane are calculated over a large range of pressure and temperature values from classical molecular dynamics simulation. We choose the constraint method of Evans and Morriss to simulate the constant-NTP ensemble. The molecular interactions are represented by Lennard-Jonnes pair potential. The computed values of diffusion coefficient and shear viscosity for liquid methane are determined in differents state points of phase diagramme. A comparison is made with the existing experimental data and for thermodynamical quantities with results computed from constant-temperature molecular dynamic simulations. The results indicate, first, constraint method do not fix the initial pressure at a prescribed value and, second, that the molecular dynamics computations with constant-pressure and constant-temperature seem an easy way to determine accurately transport properties of simple fluids.

1. Introduction.

In some situations, it is desirable to lead simulations of a fluid for the specific values of temperature and pressure under the conditions in which the energy and the volume of the fluid can fluctuate. For example, to study the diluted systems, we can simulate at the same time pure solvent and the diluted solution at the same temperature and the same pressure. This corresponds to an experimental situation in which the comparison with the calculated results of the experiment is direct [1]. Also in the study of the phase transitions of the molecular fluids, we can handle the pressure and the temperature of the simulated fluid. To complete the isothermal and isobaric conditions with the fluctuations of energy and volume, it is preferable to use a constant-pressure molecular dynamics simulation. The condition of constant pressure is carried out by surrounding the physical system with a reserve of pressure. The volume of the system changes by the movement of the piston attached to the system. The pressure takes a constant value by changing the volume of the unit cell of simulation. A constant-pressure molecular dynamics simulation is recognized to study the phase transitions. For solid state, the method of Rahman-Parrinello [2-3] is adapted best. For liquid state, the control parameters do not appear explicitly in the equations of the movement in the constraint method [4]. The condition of simulation is to maintain the initial value of the control parameters. The constraint method with constant pressure has needed a special adjustment to obtain the initial value. Generally, the extended system method [5] is recommended for constant pressure simulations. A bibliographical study lets appear that methane has been the subject of many investigations both from the experimental and the theoretical point of view [6-8]. Many studies of radiation X-ray or neutrons show that the liquid is characterized by a certain local order at short distance and is disordered at long distances. Some authors [9] have been interested in diffraction X-ray of liquid methane close to the triple point (90.7K) [9-13]. The experiment is put into practice until 92K to obtain liquid methane under a vapor pressure of saturation of 100 mmHg. At this point the density is $\rho = 0.01702 \text{ \AA}^{-3}$ and isothermal compressibility is $\beta_T = 0.145 \times 10^{-8} \text{ m}^2/\text{N}$ [12,13]. From the theoretical point of view, the equilibrium and non-equilibrium properties of methane were studied by various simulation methods, Monte Carlo (MC) [7, 8, 14] or molecular dynamics (DM) [15,16]. Different potential models were proposed [18-22] or were used to lead simulations on methane [8,23,24]. Thus, the Williams potential model of interaction site-site [17] reproduced the experimental data with a rather good precision. Most recent work [3,23,24] taking into account the quantum effects covers only some points of the phase diagram of methane and do not make it possible to approach the transport properties with a high degree of accuracy. We will undertake in this work a complete

study covering nine points of the phase diagram some of these points have been studied by constant-temperature molecular dynamics simulation in our previous work [25]. We will show that the classical approach gives very good results by molecular dynamics simulation.

2. Theory and computational details

2.1 Constraint methods

Andersen [26] proposed a molecular dynamics algorithm in which the number of particles, the temperature and the pressure (N, T, p) are independent state variables. His algorithm uses Monte-Carlo procedure to maintain the system at a constant temperature using stochastic collisions. It also uses a mathematical piston of mass M to homogeneously dilate or contract the fluid in order to keep hydrostatic pressure constant. For times shorter than the reponse time the pressure fluctuates while for longer times, the average the pressure is fixed at a desired value. The stochastic collisions which are used to maintain the system at a constant temperature involve, at intervals specified by a collision frequency, resetting particle velocities to values chosen at random from the Maxwell-Boltzmann velocity distribution. The difficulty of this algorithm is that the system trajectories through phase space are not smooth and at least for times shorter than the pressure reponse time, the pressure is not constant. Moreover, it contains two parameters (mass of the piston and the frequency of collision) which are not precisely defined. The constraint method of Evans and Morriss was conceived to figh each of these difficulties. This method does not contain indefinite parameters, the phase space trajectories are smooth and the pressure is strict constant of the motion. Their algorithm is deterministic and does not contain stochastic elements. They combined the Doll's hamiltonian for flow deformation with Gauss' principle of least constraint to develop classical equations of motion for which the temperature and hydrostatic pressure are constants of the motion [4,27-28]. These equations define a molecular dynamics algorithm for which N, T, p are the independent thermodynamic state variables.

Consider the Hamiltonian H ,

$$H = H_0 + \varepsilon \sum_{i=1}^N \dot{\mathbf{q}}_i \cdot \mathbf{p}_i \quad , \quad (1)$$

where H_0 takes the form of an equilibrium hamiltonian for a system of N particles interacting through a conservative interparticle potential $\Phi(\mathbf{q}_1, \dots, \mathbf{q}_N)$,

$$H_0 = \sum_{i=1}^N \mathbf{p}_i^2 / 2m + \Phi . \quad (2)$$

The equations of motion are:

$$\dot{\mathbf{q}}_i = \frac{\mathbf{p}_i}{m} + \varepsilon \mathbf{q}_i \quad (3)$$

$$\dot{\mathbf{p}}_i = \mathbf{F}_i - \varepsilon \mathbf{p}_i \quad (4)$$

Now if the system was *cold* ($\mathbf{p}_i = 0$ for all i), and non-interacting ($\phi_{ij}=0$), these equations would reduce to

$$\dot{\mathbf{q}}_i = \varepsilon \mathbf{q}_i \quad (5)$$

Since this equation is true for all particles i , it describes a uniform dilation or contraction of the system. This dilation or contraction is the same in each coordinate direction, so if the system initially occupied a cube of volume V , then the volume would satisfy the following equation of motion.

$$\dot{V} = 3 V \varepsilon \quad (6)$$

For *warm*, interacting systems, the equation of motion for \mathbf{q}_i shows that the canonical momentum \mathbf{p}_i is in fact peculiar with respect to the streaming velocity $d\varepsilon/dt \mathbf{q}_i$. The dissipation for the system (eq.(3) and eq.(4)) is

$$\dot{H}_0 = -\varepsilon \sum_{i=1}^N \left\{ \frac{1}{m} \mathbf{p}_i \cdot \mathbf{p}_i + \mathbf{F}_i \cdot \mathbf{q}_i \right\} = -3 p V \varepsilon \quad (7)$$

Since H_0 is the internal energy of the system we can combine eq.(7) with the equation of motion for the volume to obtain the first law of thermodynamics for adiabatic compression,

$$\dot{H}_0 = -3 p V \varepsilon = -p \dot{V} \quad (8)$$

It is worth noting that these equations are true instantaneously. One does not need to

employ any ensemble averaging to obtain eq.(8). By choosing the dilation rate $d \varepsilon/dt$ to be a sinusoidal function of time, these equations of motion can be used to calculate the bulk viscosity.

Our purposes are however to use the dilation rate as a multiplier to maintain the system at a constant hydrostatic pressure. Before we do this however, we will introduce a Gaussian thermostat into the equations of motion;

$$\dot{\mathbf{q}}_i = \frac{\mathbf{p}_i}{m} + \dot{\varepsilon} \mathbf{q}_i \quad (9)$$

$$\dot{\mathbf{p}}_i = \mathbf{F}_i - \dot{\varepsilon} \mathbf{p}_i - \alpha \mathbf{p}_i \quad (10)$$

The form for the thermostat multiplier is determined by the fact that the momenta in eq.(9) and eq.(10) are peculiar with respect to the dilating coordinate frame. By taking the moment of eq. (10) with respect to \mathbf{p}_i , and setting the time derivative of the peculiar kinetic energy to zero we observe that,

$$\alpha = -\dot{\varepsilon} + \frac{\dot{\sum_{i=1}^N \mathbf{F}_i \cdot \mathbf{p}_i}}{\sum_{i=1}^N \mathbf{p}_i^2} \quad (11)$$

Differentiating the product pV , eq.(7) with respect to time gives,

$$3\dot{p}V + 3p\dot{V} = \sum_{i=1}^N \left\{ \frac{2}{m} \dot{\mathbf{p}}_i \cdot \mathbf{p}_i + \dot{\mathbf{q}}_i \cdot \mathbf{F}_i + \mathbf{q}_i \cdot \frac{\partial \mathbf{F}_i}{\partial \mathbf{q}_i} \cdot \dot{\mathbf{q}}_i + \sum_{j \neq i} \mathbf{q}_i \cdot \frac{\partial \mathbf{F}_i}{\partial \mathbf{q}_j} \cdot \dot{\mathbf{q}}_j \right\} \quad (12)$$

The first term on the LHS is zero because the pressure is constant, and the first term on the RHS is zero because the peculiar kinetic energy is constant. Substituting the equations of motion for $d\mathbf{q}_i/dt$ and dV/dt , and we can solve for the dilation rate.

$$\dot{\varepsilon} = - \frac{\frac{1}{2m} \sum_{i \neq j}^N \mathbf{q}_{ij} \cdot \mathbf{p}_{ij} (\phi_{ij}'' + \frac{\phi_{ij}'}{q_{ij}})}{\frac{1}{2} \sum_{i \neq j}^N q_{ij}^2 (\phi_{ij}'' + \frac{\phi_{ij}'}{q_{ij}}) + 9pV} \quad (13)$$

combining this equation with eq.(11) gives a closed expression for the thermostat multiplier α . Then the pressure and the temperature will be constants of the motion. In deriving these equations we have assumed that the potential energy is pairwise additive

$$\Phi = \frac{1}{2} \sum_{i \neq j}^N \phi_{ij} \quad (14)$$

This restriction can easily be removed to allow for many body interactions. We also take \mathbf{q}_{ij} to be $\mathbf{q}_j - \mathbf{q}_i$ and similarly $\mathbf{p}_{ij} = \mathbf{p}_j - \mathbf{p}_i$.

The pressure is calculated in the usual manner, including explicitly all contributions within the potential spherical cutoff at a distance q_c and incorporating an estimated long-range corrections calculated as follows. The virial contribution to the pressure from outside the spherical cutoff is given by

$$\begin{aligned} w_{q>q_c} &= \sum_{\substack{i<j \\ |q_{ij}|>q_c}}^N \mathbf{q}_{ij} \cdot \phi'_{ij} \\ &= 2\pi\rho N \int_{q_c}^{\infty} dq q^3 \phi' g(q) \end{aligned} \quad (15)$$

ρ is the density of the fluid . Approximating the pair distribution function $g(q)$ by unity the long-range corrections to the virial for the Lennard-Jones potential is

$$w_{q>q_c} = 16\pi\rho N \varepsilon_{LJ} \left[\frac{2}{3} (\sigma/q_c)^9 - (\sigma/q_c)^3 \right], \quad (16)$$

and the Lennard-Jones potential is given by

$$\phi(q) = 4\varepsilon_{LJ} \left[(\sigma/q)^{12} - (\sigma/q)^6 \right] \quad (17)$$

specified by the parameters ε_{LJ} and σ . The total pressure is then given by

$$p = \rho k_B T - (1/3V) (w_{q<q_c} + w_{q>q_c}) \quad (18)$$

In order to maintain consistency it is necessary to include long-range correction to the denominator of $\dot{\varepsilon}$ in eq.(13). This can be calculated in the same way as the virial long-range correction. If

$$\begin{aligned}\chi_{LRC} &= \frac{1}{2} \sum_{\substack{i,j \\ q_{ij} > q_c}}^N q_{ij}^2 (\phi_{ij}'' + \phi_{ij}'/q_{ij}) \\ &= 2\pi\rho N \int_{q_c}^{\infty} dq q^4 (\phi'' + \phi'/q) g(q)\end{aligned}\quad (19)$$

We may again approximate $g(q)$ by unity and for the Lennard-Jones potential we have

$$\chi_{LRC} = 96\pi\rho N \varepsilon_{LJ} \left[\frac{4}{3} (\sigma/q_c)^9 - (\sigma/q_c)^3 \right] \quad (20)$$

The long-range correction to the numerator of eq.(13) is zero as at any point on the spherical cutoff the direction of \mathbf{p}_{ij} is random. Substituting eq.(20) into eq.(13) the expression for $\dot{\varepsilon}$ becomes

$$\dot{\varepsilon} = - \frac{\frac{1}{2m} \sum_{i \neq j}^N \mathbf{q}_{ij} \cdot \mathbf{p}_{ij} (\phi_{ij}'' + \frac{\phi_{ij}'}{q_{ij}})}{\frac{1}{2} \sum_{i \neq j}^N q_{ij}^2 (\phi_{ij}'' + \frac{\phi_{ij}'}{q_{ij}}) + \chi_{LRC} + 9pV} \quad (21)$$

The constraint equations (11) and (13) are switched on at some point in the simulation usually in the equilibration stage. These constraints then act to fix the temperature and pressure at their values at that instant.

2.2 Starting parameters and algorithms

Isothermal-isobaric molecular dynamics calculations were performed on a sample of size $N = 864$ molecules of masse m . The molecules interact by Lennard-Jones pair

Table 1: Type of fluids with the value of the Lennard-Jones parameters, and thermodynamic state points investigated in this work. Densities, temperatures and pressures are in real and reduced units.

State Point	System	T (K ^o)	T*	ρ (g/cm ³)	ρ^*	p (bar)	p*	σ/A^o	ϵ/k_B	m/amu
Msp1[8]	CH ₄ (l)	91.0	0.6103	0.4495	0.8851	9.52	0.024	3.743[7]	149.1[7]	16.04303
Msp2	CH ₄ (l)	99.8	0.6692	0.4407	0.8678	26.68	0.068			
Msp3	CH ₄ (l)	105.4	0.7069	0.4331	0.8528	0.78	0.002			
Msp4[8]	CH ₄ (l)	108.0	0.7243	0.4263	0.8394	38.84	0.099			
Msp5	CH ₄ (l)	110.9	0.7437	0.4253	0.8375	16.08	0.041			
Msp6	CH ₄ (l)	116.5	0.7813	0.4173	0.8217	27.29	0.070			
Msp7	CH ₄ (l)	122.1	0.8189	0.4091	0.8056	32.56	0.083			
Msp8[8]	CH ₄ (l)	125.0	0.8384	0.4005	0.7887	63.56	0.162			
Msp9	CH ₄ (l)	127.6	0.8558	0.4006	0.7888	52.05	0.134			

potential (eq.(17)). The units of energy, length, and mass were chosen to be, respectively ϵ_{LJ} , σ , and m . The corresponding microscopic time scale is $\tau = (m\sigma^2/\epsilon_{LJ})^{1/2}$. The state of our system is specified through the reduced number density and temperature $\rho^* = \rho\sigma^3$, $T^* = k_B T/\epsilon_{LJ}$ and $p^* = p\epsilon_{LJ}\sigma^{-3}$. The thermodynamic state points sp (ρ , T) of the systems of liquid methane are summarized in table 1. The sp (Msp1, Msp4, Msp8) were taken from Sesé's work [8]. The other state points were taken from Tchouar and al studies [25]. The equations of motion were solved using the Gear Predictor integration scheme with a constant time step algorithm ($\Delta t = 0.5 \times 10^{-14}$ s) and wherein the temperature T and the pressure were kept constants by the constraint method of Evans and Morriss [4]. The pressures chosen in these calculations are the equilibrium pressures obtained in constant-temperature molecular dynamic simulations given by the work of Tchouar and al [25]. Periodic boundary conditions around the central cubic box and the minimum image truncation were included to perform calculations. Continuum corrections to configurational energies and pressures have also been included. In the simulation of Lennard-Jones particles, the value of a spherical cutoff is $q_c = 2.5\sigma$ referred by Allen and Tildesley [29].

The starting configuration is face-centred cubic (FCC) lattice for molecule positions. Initial molecular velocities were obtained from the Maxwell-Boltzmann distribution. The equilibration period is extended up to duration of 20 ps. The production phase of data, starting after the equilibration, goes on for 100 ps in order to increase the accuracy of the stress autocorrelation function. The error bars for the thermodynamic quantities and the pair distribution functions have been calculated.

The self-diffusion coefficient D of a particle is evaluated by the Einstein formulas [29]:

$$D = \frac{1}{6N} \lim_{t \rightarrow \infty} \frac{d}{dt} \left\langle \sum_i^N [\mathbf{q}_i(t) - \mathbf{q}_i(0)]^2 \right\rangle, \quad (22)$$

where $\mathbf{q}_i(t)$ are the positions of the particles at time t . D is proportional to the slope of the mean-square displacement at long times [29].

The shear viscosity coefficient η can be evaluated from both Green-Kubo and generalized formulas [30]. For soft-body potentials, most simulators have used the Green-Kubo equation [29], which is an integral over the stress autocorrelation function,

$$\eta_{xy} = 1/Vk_B T \int_0^\infty \langle J_{xy}(t) \cdot J_{xy}(0) \rangle dt. \quad (23)$$

The component of the microscopic stress tensor is given by

$$J_{xy}(t) = \sum_{i=1}^N \left(m p_i^x p_i^y - \frac{1}{2} \sum_{i \neq j} \frac{q_{ij}^x q_{ij}^y}{q_{ij}} \frac{\partial \phi_{ij}}{\partial q_{ij}} \right). \quad (24)$$

The stress autocorrelation function necessarily involves the entire system; consequently, we cannot improve the statistical precision of results for viscosity by averaging over the N particles in the system. However, for stationary, homogeneous, uniform fluids, the statistical precision can be improved somewhat by averaging over all three terms that result from the stress tensor,

$$\eta = \frac{1}{3} (\eta_{xy} + \eta_{yz} + \eta_{zx}). \quad (25)$$

3. Results

3.1 Pair distribution functions

Structural information is illustrated by figure 1 for three points Msp1, Msp6 and Msp9. The $g(q)$ obtained takes a well defined form and these oscillations correspond to that of a liquid for all the points.

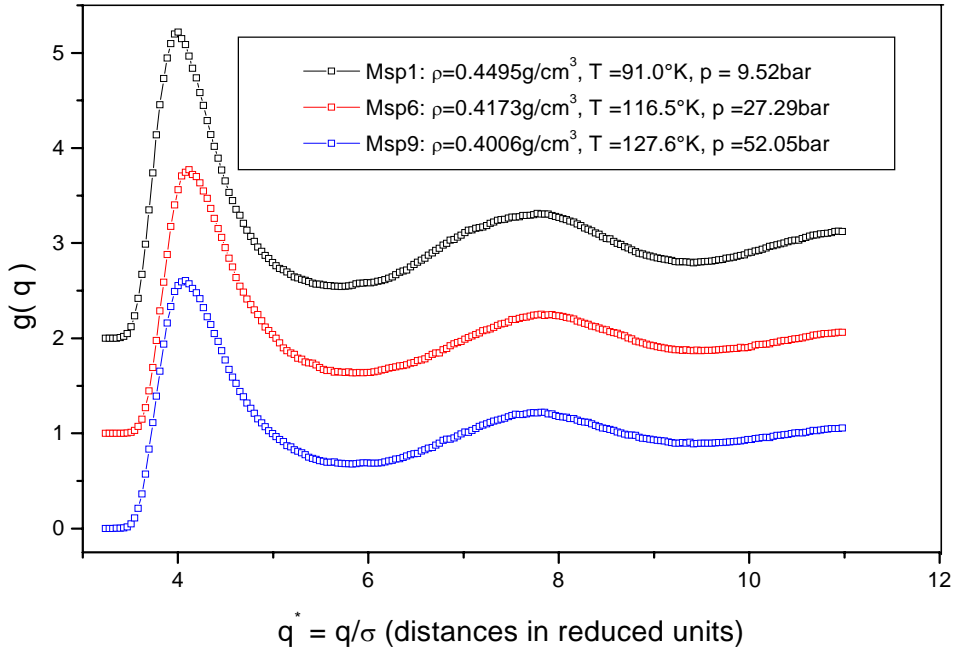


Figure 1: Pair distribution function for three points of the phase diagram Msp1, Msp6 and Msp9 in constant-pressure molecular dynamics simulation.

The average number of neighbours for a methane molecule is obtained from

$$n(R) = 4\pi\rho \int_0^R q^2 g(q) dq, \quad (26)$$

where the integration limit R is taken as the position of the successive minima in $g(q)$. The analysis of these curves enables us to calculate the position of the various peaks and the number of nearest neighbours close to a molecule of reference deferred in table 2.

Table 2: Position of the peaks in the radial distribution function and number of nearest neighbours in constant-pressure molecular dynamics simulation.

	Msp1	Msp2	Msp3	Msp4	Msp5	Msp6	Msp7	Msp8	Msp9
R_{max1}/ Å	4.05	4.05	4.05	4.05	4.05	4.05	4.05	4.05	4.05
R_{min1}/ Å	5.75	5.75	5.75	5.75	5.75	5.85	5.85	5.85	5.85
R_{max2}/ Å	7.75	7.75	7.75	7.75	7.75	7.75	7.75	7.75	7.75
R_{min2}/ Å	9.52	9.52	9.52	9.52	9.52	9.55	9.55	9.55	9.55
Number of nearest neighbours (max1)	11.38	11.38	11.89	11.73	11.55	11.42	11.30	11.02	11.12
Number of nearest neighbours (max2)	54.77	53.08	52.72	51.49	51.63	49.48	48.80	48.28	48.11

At the temperature $T = 92^\circ\text{k}$, $g(r)$ measured by X-rays diffraction gives the number of nearest neighbours of the first peak equal to "12 and number of nearest neighbours of the second peak equal to" 55 [31] by using the same procedure of integration as our work. Our values are close to the experimental values this shows the reliability of the potential used.

3.2 Thermodynamic and transport quantities:

To lead to a better comprehension of our results, we considered it useful to give the evolution of the thermodynamic properties in time in figures 2, 3, 4 and 5. Essential characteristics can be draw from these figures. Since the temperature increases, the total energy increases and the fluctuations are significant. With the enthalpy, we confirm that this effect of the temperature and the fluctuations are more remarkable and considerable. For volume, the fluctuations are small with decreasing temperature. In order to obtain a better synthesis of our results, we choose to join together the data obtained in constant-temperature molecular dynamic simulations [25] in table 3.

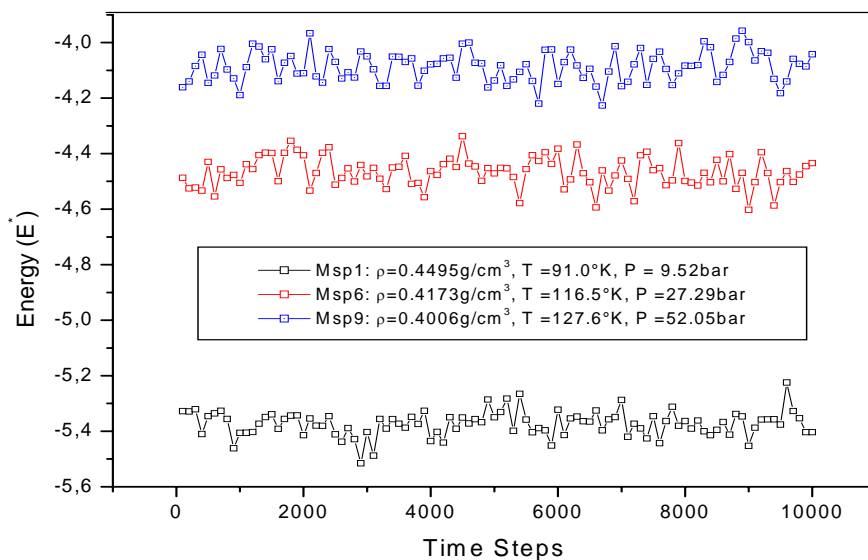


Figure 2: Total energy as a function of time steps in constant-pressure molecular dynamics simulation.

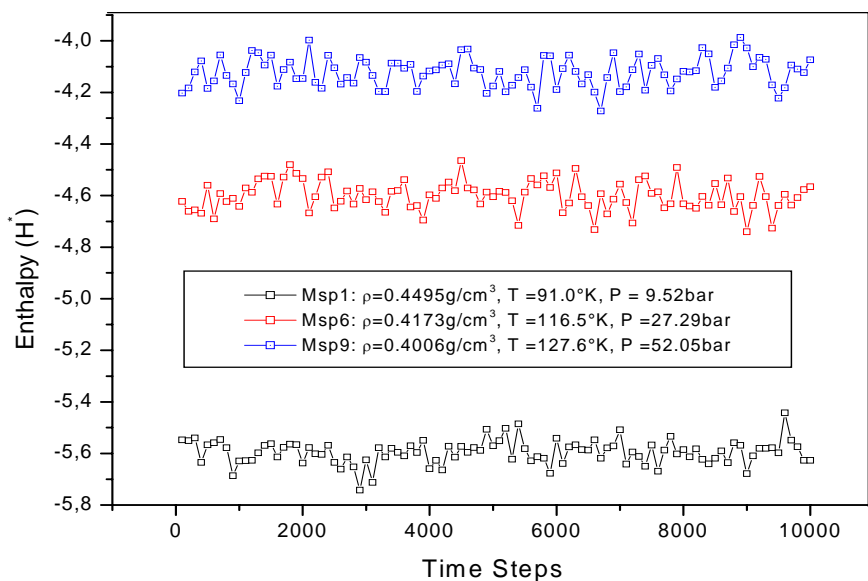


Figure 3: Enthalpy as a function of time steps in constant-pressure molecular dynamics simulation.

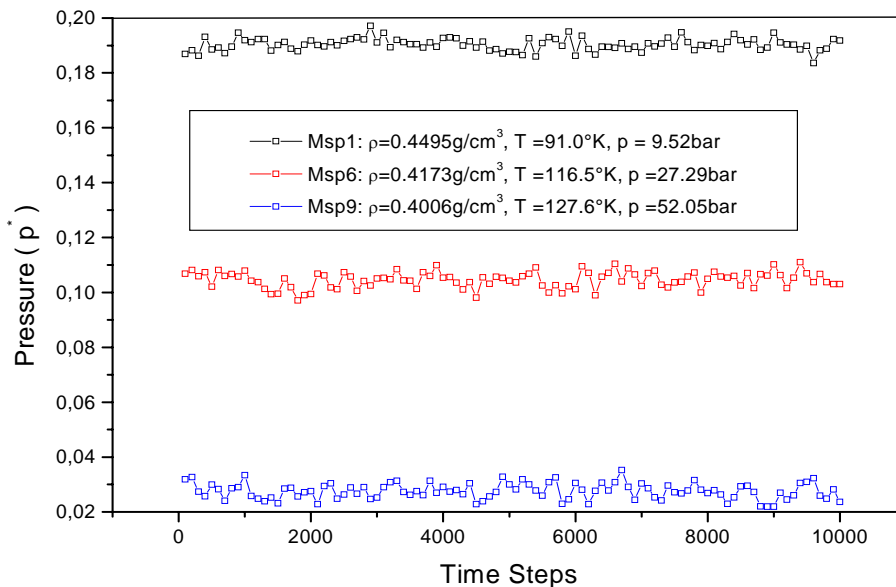


Figure 4: Pressure as a function of time steps in constant-pressure molecular dynamics simulation.

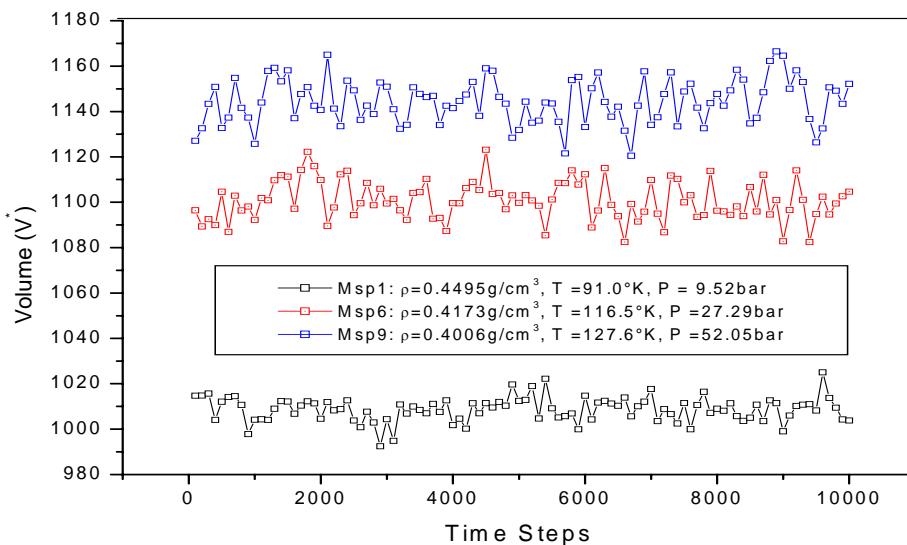


Figure 5: Volume as a function of time steps in constant-pressure molecular dynamics simulation.

Table 3: Thermodynamic properties of liquid methane calculated in constant-pressure molecular dynamics simulation in reduced units. Constant-temperature molecular dynamics data are reported as well.

Configurational energy $U^*=U/N\varepsilon_{LJ}$, Total energy $E^*=E/N\varepsilon_{LJ}$, Pressure $p^*=p\varepsilon_{LJ}\sigma^{-3}$, Enthalpy $H^*=H/N\varepsilon$, Self-Diffusion Coefficient $D^*=D\sqrt{m/\varepsilon_{LJ}}/\sigma$, Shear Viscosity $\eta^*=\eta\sigma^3/\varepsilon_{LJ}\tau$.

State point	Method	U^*	E^*	p^*	H^*	D^*	η^*
Msp1	MDNTp ^(a)	-6.286 ± 0.060	-5.371 ± 0.067	0.188 ± 0.133	-5.591 ± 0.191	0.024	2.58
	MDNVT ^(b)	-6.460 ± 0.059	-5.541 ± 0.112	0.024 ± 0.245	-5.513 ± 0.144	0.018	5.44
Msp2	MDNTp ^(a)	-6.073 ± 0.043	-5.069 ± 0.045	0.134 ± 0.046	-5.231 ± 0.077	0.034	2.67
	MDNVT ^(b)	-6.282 ± 0.034	-5.275 ± 0.082	0.068 ± 0.139	-5.197 ± 0.206	0.026	5.40
Msp3	MDNTp ^(a)	-5.907 ± 0.044	-4.847 ± 0.046	0.185 ± 0.008	-5.074 ± 0.047	0.043	2.33
	MDNVT ^(b)	-6.154 ± 0.024	-5.092 ± 0.026	0.002 ± 0.109	-5.096 ± 0.153	0.035	3.55
Msp4	MDNTp ^(a)	-5.878 ± 0.049	-4.792 ± 0.050	0.088 ± 0.005	-4.900 ± 0.055	0.046	2.31
	MDNVT ^(b)	-6.049 ± 0.024	-4.962 ± 0.029	0.099 ± 0.116	-5.080 ± 0.164	0.038	2.94
Msp5	MDNTp ^(a)	-5.770 ± 0.056	-4.655 ± 0.054	0.140 ± 0.006	-4.830 ± 0.057	0.049	2.02
	MDNVT ^(b)	-6.016 ± 0.020	-4.900 ± 0.023	0.041 ± 0.108	-4.949 ± 0.154	0.041	2.77
Msp6	MDNTp ^(a)	-5.639 ± 0.053	-4.467 ± 0.053	0.104 ± 0.007	-4.600 ± 0.054	0.058	1.88
	MDNVT ^(b)	-5.879 ± 0.028	-4.705 ± 0.025	0.070 ± 0.112	-4.791 ± 0.163	0.048	2.47
Msp7	MDNTp ^(a)	-5.474 ± 0.062	-4.245 ± 0.062	0.082 ± 0.004	-4.354 ± 0.064	0.067	1.54
	MDNVT ^(b)	-5.735 ± 0.029	-4.506 ± 0.027	0.083 ± 0.112	-4.610 ± 0.165	0.055	1.90
Msp8	MDNTp ^(a)	-5.439 ± 0.057	-4.181 ± 0.057	0.020 ± 0.003	-4.208 ± 0.060	0.069	2.13
	MDNVT ^(b)	-5.606 ± 0.026	-4.348 ± 0.026	0.162 ± 0.086	-4.554 ± 0.134	0.061	2.07
Msp9	MDNTp ^(a)	-5.371 ± 0.053	-4.088 ± 0.057	0.027 ± 0.005	-4.124 ± 0.060	0.074	1.71
	MDNVT ^(b)	-5.596 ± 0.025	-4.312 ± 0.026	0.134 ± 0.103	-4.482 ± 0.157	0.063	2.26

a) Our work

b) Taken from [25].

Significant conclusions can be deduced from this table. By traversing all the points from Msp1 to Msp9, it is to be noticed that an increase in the temperature generates an

increase in configurational energy and total energy with an irregularity in the fluctuations. From Msp1 to Msp9, the enthalpy fluctuations do not show significant changes. Generally, the pressure fluctuations are constant for all the points. By comparing the two methods, the fluctuations are large for U^* and E^* , on the other hand they are small for p^* and H^* for MDNTp compared to MDNVT. In the light of the foregoing discussion, MDNTp error bars on total and configurational energies are larger than in constant-temperature molecular dynamic simulations, except for Msp1 and Msp2, but error bars on pressure and enthalpy are smaller for all the points. The diffusion coefficients and shear viscosity values show that our system is in a liquid state compared to MDNVT. The most significant remark is that the constraint method has many difficulties to maintain the initial pressures at prescribed values given by MDNVT. We can conclude that we are treating another equilibrium state. The activation energy can be extracted from the diffusion coefficient versus the temperature by using the Arrhenius law as illustrated in figure 5.

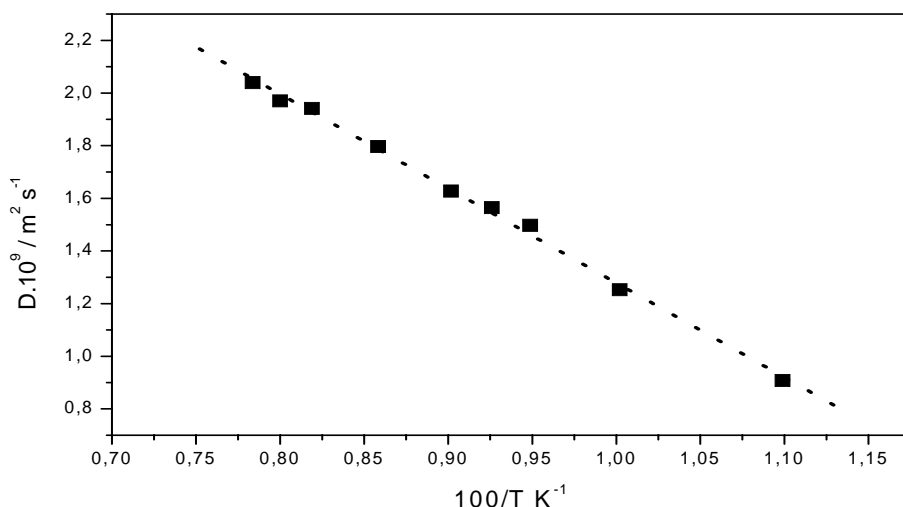


Figure 5: Diffusion coefficient versus temperature in constant- pressure molecular dynamics simulation

The value of the activation energy measured by NMR is equal 3.7 K.J.mol^{-1} [32] and our value is equal $2.984 \text{ K.J.mol}^{-1}$ for MDNTp. We point out that the value obtained starting from a simulation MDNVT is $3.34 \text{ K.J.mol}^{-1}$ [25]. This value is closer to the experimental activation energy compared to a MDNTp.

4. Conclusion

It comes out from this study that classical approach is sufficient to study the properties of liquid methane in an unspecified point of the phase diagram. A complete study of these properties can be undertaken in constant-pressure molecular dynamics simulation. Taking into account our results, we think that the constraint method of Evan and Morriss is a purely mathematical and logical approach missing physical direction, the initial pressure not being maintained. It would be useful to lead simulations to constant pressure with the extended system method by checking the assumption of Nosé [5] and by carrying out simulation experiments at constant pressure for molecular systems with interactions site-site.

References.

1. Owicki, J.; and Scheraga, H. A. *J. Am. Chem. Soc.* **1977**, *99*, 7413.
2. Parrinello, M.; and Rahman, A. *Phys. Rev. Lett.* **1980**, *45*, 1196.
3. Parrinello, M.; and Rahman, A. *J. Appl. Phys.* **1981**, *52*, 7182.
4. Evans, D. J.; and Morriss, G. P. *Chem. Phys.* **1983**, *77*, 63.
5. Nosé, S.; *In Computer Simulation in Materials Science*, Kluwer Academic Publishers : Netherlands, **1991**.
6. Seitz, J. C.; and Blancor, J. G. *J. Chem. Thermodynamics.* **1996**, *28*, 1207-1213.
7. Mc Donald, I. R.; and Singer, K. *Molec. Phys.* **1972**, *23*, 29.
8. Sesé, L. M. *Molec. Phys.* **1992**, *76*, 1335-1346.
9. Habenschuss, A.; Johnson, E.; and Narten, A. H. *J. Chem. Phys.* **1981**, *74*, 5234.
10. Matheson Company, Inc., East Rutherford, N. J. 07073.
11. Displex Closed-Cycle Refrigeration Unit, Air Products and Chemicals, Inc., Allentown, Pa. 18103.
12. Rowlinson, J. S. *Liquids and Liquid Mixtures*, 2nd ed; Butterworths: London, 1969; p 51.
13. Narten, A. H.; and Levy, H. A. In *waters : A Comprehensive Treatise*; Franks, F., ed.; Plenum : New York, 1972; Vol. 1, p 314.
14. Kincaid, R. H.; and Scheraga, H. A. *J. Phys. Chem.* **1982**, *86*, 838.
15. Murad, S.; Evans, D. J.; Gubbins, K. E.; Street, W. B.; and Tildesley, D. J. *Molec. Phys.* **1979**, *37*, 725.
16. Schoen, M.; Hoheisel, C.; and Beyer, O. *Molec. Phys.* **1986**, *58*, 699.
17. Williams, D. E. *J. Chem. Phys.* **1967**, *47*, 4680.
18. Catlow. C. R. A.; Harker. A. H.; and Hayns. M. R. *J. Chem. Soc. Faraday Trans.* **1975**, *71*, 275.
19. Kolos. W.; Raghino. G.; Clementi. E.; and Novaro. O. *Int. J. Quantum*

- Chem.* **1980**, *17*, 429.
20. Bohm. H. J.; Ahlrichs. R.; Scharpe. P.; and Shiffer. H. *J. Chem. Phys.* **1984**, *81*, 1389.
 21. Gianturco. F. A. *Molec. Phys.* **1995**, *84*, 481.
 22. Schindler, H.; Vogelsang. R.; Staemmler. V.; Siddiqi. M. A.; and Svejda. P. *Molec. Phys.* **1993**, *80*, 1413.
 23. Nagy, J.; Weaver, D. F.; and Smith, Jr., V. H. *J. Phys. Chem.* **1995**, *99*, 8058.
 24. Nagy, J.; Weaver, D. F.; and Smith, Jr., V. H. *Molec. Phys.* **1995**, *85*, 1179.
 25. Tchouar, N.; Benyettou, M.; and Ould Kadour, F. *Int. J. Mol. Sci.* **2003**, *4*, 595.
 26. Anderson, H.C. *J. Chem. Phys.* **1980**, *72*, 2384.
 27. Evans, D. J.; and Morriss, G. P. *Phys. Rev. A.* **1984**, *30*, 1528.
 28. Evans, D. J.; and Morriss, G. P. In *Statistical Mechanics of NonEquilibrium Liquids* Academic Press : London, **1990**.
 29. Allen, M.; and Tildesley, D. In *Computer Simulation of liquids* Oxford University Press : Oxford, **1987**.
 30. Hansen, J. P.; and Mc Donald, I.R. In *Theory of simple liquids* Academic Press : London, **1986**.
 31. Habenschuss, A.; Johnson, E.; and Narten, A. H. *J. Chem. Phys.* **1981**, *74*, 5234.
 32. Haertel, K. **1984**, Thesis Bochum.